International Journal of Chronic Obstructive Pulmonary Disease Dovepress
open access to scientific and medical research
Open Access Full Text Article
ORIGINAL RESEARCH

Histone Deacetylase 2 Suppresses Skeletal Muscle Atrophy and Senescence via NF-κB Signaling Pathway in Cigarette Smoke-Induced Mice with Emphysema

Chao Li
Zhaohui Deng
Guixian Zheng
Ting Xie
Xinyan Wei
Zengyu Huo
Jing Bai

Department of Respiratory Medicine, The First Affiliated Hospital of Guangxi Medical University, Nanning, Guangxi, 530021, People's Republic of China

Background: Exposure to cigarette smoke (CS) is the main risk factor for chronic obstructive pulmonary disease (COPD). CS not only causes chronic airway inflammation and lung damage but also is involved in skeletal muscle dysfunction (SMD). Previous studies have shown that histone deacetylase 2 (HDAC2) plays an important role in the progression of COPD. The aim of this study was to determine the role of HDAC2 in CS-induced skeletal muscle atrophy and senescence.

Methods: Gastrocnemius muscle weight and cross-sectional area (CSA) were measured in mice with CS-induced emphysema, and changes in the expression of atrophy-related markers and senescence-related markers were detected. In addition, the relationship between HDAC2 expression and skeletal muscle atrophy and senescence was also investigated.

Results: Mice exposed to CS for 24 weeks developed emphysema and gastrocnemius atrophy and exhibited a decrease in gastrocnemius weight and skeletal muscle cross-sectional area. In addition, the HDAC2 protein levels were significantly decreased while the levels of atrophy-associated markers, including MURF1 and MAFbx, and senescence-associated markers, including P53 and P21, were significantly increased in the gastrocnemius muscle. In vitro, the exposure of C2C12 cells to cigarette smoke extract (CSE) significantly increased the MAFbx and MURF1 protein levels and decreased the HDAC2 protein levels. Moreover, overexpression of HDAC2 significantly ameliorated CSE-induced atrophy and senescence and reversed the increased MURF1, MAFbx, P53, and P21 expression in C2C12 cells. In addition, CSE treatment significantly increased the IKK and NF-κB p65 protein levels, and PTDC (an NF-kB inhibitor) ameliorated atrophy and senescence.

Conclusion: Our findings suggest that HDAC2 plays an important role in CS-induced skeletal muscle atrophy and senescence, possibly through the NF-κB pathway.

Keywords: histone deacetylase 2, skeletal muscle, atrophy, senescence, nuclear factor-κB

Introduction

Chronic obstructive pulmonary disease (COPD) is not a simple pulmonary disease but a chronic systemic inflammatory disease that is simultaneously mediated by multiple risk factors and biological mechanisms, and COPD has significant extra-pulmonary manifestations.[1] Skeletal muscle dysfunction (SMD) is common in patients with COPD and is strongly associated with quality of life and exacerbation of disease.[2] SMD is mainly characterized by decreased skeletal muscle endurance

Correspondence: Jing Bai
The First Affiliated Hospital of Guangxi Medical University, No. 6 Shuangyong Road, Nanning, Guangxi
Tel +86-771-5356702
Fax +86-771-5608132
Email bj1312002@aliyun.com

Received: 7 April 2021
Accepted: 20 May 2021
Published: 4 June 2021

and muscle strength as well as increased susceptibility to fatigue during exercise.[3] In addition, SMD has been observed in nonsymptomatic human smokers and animals exposed to cigarette smoke without overt pulmonary disorders.[4] Although it has been demonstrated that rehabilitation exercises,[5] nutritional support,[6] and neuromuscular electrical stimulation[7] improve the quality of life of COPD patients, there are still several limitations to the current treatments for SMD.

Exposure to cigarette smoke (CS) is the most important risk factor for COPD; it not only causes chronic airway inflammation and lung damage[8] but also is involved in the development of SMD.[9] Skeletal muscle atrophy is caused by an imbalance between muscle protein synthesis and degradation.[10] The ubiquitin-proteasome system (UPS) and the autophagic lysosomal pathway are the two major intracellular protein degradation pathways, and they are functionally complementary and interconnected.[11–13] The UPS is an ATP-dependent protein hydrolysis system that degrades target proteins to which ubiquitin is coupled. The most critical molecules in this system are E3 ligase muscle ring finger gene 1 (MURF1) and muscle atrophy F-box (MAFbx). These proteins are primarily expressed in muscle tissues, and their expression levels in skeletal muscle are significantly increased in response to multiple stressors that induce skeletal muscle atrophy. More importantly, the suppression or complete inhibition of MURF1 and MAFbx expression results in muscle sparing in multiple atrophy.[14] Therefore, these proteins have been associated with the regulation of skeletal muscle atrophy under various pathophysiological conditions and have been identified as excellent markers of muscle atrophy.[15–17] However, the mechanism by which MURF1 and MAFbx regulate CS-induced skeletal muscle atrophy has not yet been identified.

Inflammation is involved in the progression of SMD via the regulation of skeletal muscle atrophy and senescence. Our previous study showed that histone deacetylase 2 (HDAC2) mediates CS-induced inflammatory responses in skeletal muscle.[18,19] HDAC2 is a class I HDAC that can deacetylate histone proteins and non-histone proteins (eg, NF-κB).[20] HDAC2 acts as a repressor of gene expression by promoting a closed chromatin conformation.[21] Previous studies have shown that HDAC2 is involved in the regulation of a variety of cellular activities, such as cell cycle progression, cell proliferation, differentiation, inflammation, and glucocorticoid receptor function,[22] and HDAC2 plays an important role in chronic lung inflammatory diseases, such as COPD, asthma, and pulmonary fibrosis.[23–26] The expression and activity of HDAC2 in the lungs of patients with COPD are reduced, and this decreased HDAC2 expression is associated with glucocorticoid resistance.[27] Moreover, studies shown that the activity of HDACs in the lung parenchyma of COPD patients is significantly decreased; the degree of decrease is related to the severity of the disease and the degree of inflammation, and the most significant decrease is observed in the activity of HDAC2, which accounts for more than 95% of the decreased HDAC activity in severe COPD patients.[28] Masako observed a significant decrease in HDAC2 expression in the quadriceps muscles of COPD patients compared to the quadriceps muscles of normal subjects; HDAC2 expression was associated with NF-κB activity and TNF-α expression.[29] These results suggest that HDAC2 is involved in the inflammatory response and skeletal muscle atrophy.

In the present study, we investigated the effects of HDAC2 on CS-induced skeletal muscle atrophy and senescence in vivo and in vitro and explored its possible mechanisms of action.

Materials and Methods

CS-Induced Emphysema Mice Model

A total of 32 male C57BL/6 mice (14±2 g, 3–4 weeks) were obtained from the Center of Guangxi Medical University, China. All the animals were housed in an environment with a temperature of 22 ± 1°C, a relative humidity of 50 ± 1%, and a light/dark cycle of 12/12 hours. All the animal studies (including the mouse euthanasia procedure) were performed in compliance with the regulations and guidelines of Guangxi Medical University institutional animal care and conducted according to the AAALAC and IACUC guidelines.

The mice were randomly divided into two groups: the control group (N) and the experimental group (COPD). The control group (n=16) was exposed to room air, and the experimental group (n=16) was exposed to cigarette smoke for 12 or 24 weeks, according to a previous report.[30] Briefly, the COPD group was exposed to an amount of CS equivalent to smoking 5 cigarettes for 1 hour each time (4 times/day, 6 days/week), while the N group was placed in another glass chamber and housed normally and exposed to air under the same conditions. At the end of the experiment, the mice were anaesthetized with sodium pentobarbital (40 mg/kg) by intraperitoneal injection. All the mice were sacrificed by exsanguination, and the gastrocnemius muscle was weighed. The lung and

gastrocnemius muscle were completely removed and placed on ice. The right lung tissue and right gastrocnemius muscle were then embedded and sectioned for histological examination. The other side of the gastrocnemius muscle was frozen in liquid nitrogen for use in Western blotting or RT-PCR analysis.

Histology

Lung tissue and gastrocnemius muscle were fixed in 10% formalin (>4 volumes of each sample) at room temperature overnight. The samples were then paraffin-embedded and sectioned (4 μm). The sections were stained with haematoxylin staining solution for 5 min, washed once with water, incubated in 95% ethanol for 5 seconds, and stained in eosin solution for 1 min. The sections were then incubated in 95% ethanol for 2 min, transferred to xylene, sealed, and observed under a microscope (Olympus, Japan). The mean linear intercept of the alveolar space (MLI) and the cross-sectional area of the gastrocnemius muscle (CSA) were analysed and quantified using a blinded method, as previously described.[31,32] Briefly, the MLI was assessed based on the number of alveolar septa (L/Ns), and the CSA was assessed based on morphological analysis of the gastrocnemius muscle by H&E staining. Three slices per mouse were chosen, and 2–3 random fields of view of each slice were analysed. All the results were evaluated with ImageJ software.

Western Blotting

C2C12 cells and gastrocnemius muscle were lysed with RIPA buffer (Solarbio, Beijing, China); the protein concentrations were measured by a BCA kit (Beyotime, Shanghai, China). Then, 40 μg of the samples were electrophoresed in 10–12% SDS polyacrylamide gels and electrically transferred to 0.2-μm PVDF membranes (Millipore, USA). The membranes were immersed and incubated in 5% fat-free milk at room temperature for 1 hour. The membranes were then incubated with primary antibodies against HDAC2, P53, P21, IKK, and NF-κBp65 (1:1000, Cell Signaling Technology, USA) and MURF1, MAFbx, and SMP30 (1:1000, Abcam, UK) overnight at 4°C, followed by incubation with fluorescent secondary antibodies (1:1000, Cell Signaling Technology, USA). The GAPDH antibody (1:1000, Cell Signaling Technology, USA) was used as the control. Fluorescence signal detection was performed with an infrared imaging instrument (Odyssey, USA), and protein expression was quantified by densitometry analysis with ImageJ software.

Cell Culture

Murine skeletal muscle C2C12 cells were obtained from the Type Culture Collection of the Chinese Academy of Sciences, Shanghai, China. The cells were cultured in Dulbecco's modified Eagle medium (DMEM) (Gibco, Shanghai, China) containing 10% inactivated foetal bovine serum (FBS), 2 mM glutamine, 0.5% antimycoplasma, and 1% antibiotics in a humidified atmosphere containing 5% CO2/95% air at 37°C. When cell confluence reached 80%, cell differentiation was induced by incubation with 2% horse serum for 6 days. The completely differentiated cells were treated with various concentrations of CSE for 24 hours. Then, the cells transfected with lentivirus and treated with PDTC (20 μM, Abmole, USA) before being stimulated with for 24 hours. Cells in passages 3–8 were used in these experiments.

Cigarette Smoke Extract Preparation

CSE was prepared following the methods described in a previous study.[33] Briefly, ten cigarettes (Guangxi, China) were drawn with a syringe and shaken so that the smoke could be uniformly dissolved in 10 mL PBS, and the CSE was filtered twice through a 0.22-μm filter membrane (Millipore, USA). The CSE concentration was measured at 320 nm using a NanoDrop, and the solution obtained was considered the working solution. Then, the cells were diluted to various concentrations (0, 0.01, 0.1 −0.3%) in foetal bovine serum (FBS)-free DMEM (Gibco, Shanghai, China).

Lentivirus Transfection

A total of 3×10^5 C2C12 cells were seeded into 6-well plates and incubated in 10% FBS DMEM at 37°C for 16–24 hours until the cell confluence reached 20–30%. Then, lentivirus was added for transfection. Lentivirus synthesis and design were performed by a specialized company (GeneChem, Shanghai, China). Forward primer:

5′-AGGTCGACTCTAGAGGATCCCGCCACCATG GCGTACAGTCAAGGAGG-3′. Reverse primer:

5′-TCCTTGTAGTCCATACCAGGGTTGCTGAGTT GTTCTGACTTGGCTC-3′.

The cells were infected at an MOI of 75 and under HiTransG P solution conditions for 24 hours. The cell growth status was observed after changing the medium; the transfection efficiency was observed under a fluorescence microscope (Olympus CKX53, Japan). The cells were then cultured in 10% FBS DMEM containing 0.5 μg/mL puromycin, and the

medium was changed every 2–3 days until the cells in the lentiviral group were completely resistant. C2C12 cells were differentiated in 2% horse serum-containing medium for 6 days and then incubated in medium with or without 0.3% CSE for 24 hours, and the cells were collected for further analysis.

Immunofluorescence Staining

C2C12 cells were stimulated with or without 0.3% CSE for 24 hours. The cells were then washed three times with PBS in 24-well plates, fixed with 4% paraformaldehyde for 15 min, and mixed with 0.5% Triton X-100 for 20 min at room temperature. Consequently, the samples were mixed with 5% BSA at 37°C for 30 min and then incubated with primary anti-MHC antibodies (1:200, Santa Cruz, USA) at 4°C overnight and with fluorescent mouse antibodies (1:250, Cell Signaling Technology, USA) at 37°C for 30 min. Finally, the samples were stained with DAPI (Solarbio, Beijing, China) for 5 min in the dark. The images were collected under a fluorescence microscope (Olympus CKX53, Japan). The image results were quantified using ImageJ software to analyse the myotube parameters. The mean myotube diameter was calculated as the mean of five approximately isometric measurements performed along the length of the myotube. Five fields of view were randomly selected for each group, and 10–15 myotubes were measured per field of view.

SA-β Gal Staining

C2C12 cells were differentiated for 6 days in 6-well plates and then treated with or without 0.3% CSE stimulation for 24 hours, according to the manufacturer's instructions (GENMED, Shanghai, China). Briefly, C2C12 cells were washed two times with PBS and then incubated with GENMED clean-up solution (Reagent A) (1 mL/well, 1 mL GENMED fixative (Reagent B) and GENMED clean-up solution (Reagent C), which were added separately. Then, the cells were incubated fixed for 5 min at room temperature, and sufficient volumes of Reagent D and Reagent E were added and incubated at 37°C for 12 hours in the dark. Positive cells (blue cells) were observed under a microscope and photographed (Olympus, Japan), and 5 fields of view per group were analysed. Positive cell expression was calculated using ImageJ software.

Real Time-PCR

Total RNA was extracted with TRIzol (Invitrogen) and reverse transcribed into cDNA using a reverse transcription kit (Promega, USA) according to the manufacturer's instructions. RT-PCR was performed using a SYBR® Premix Ex Taq II kit (Takara, Japan). The amplification conditions were as follows: denaturation at 95°C for 30 seconds, annealing at 95°C for 5 seconds, and extension at 60°C for 34 seconds. The PCR primer sequences are shown in Table 1. GAPDH was used as a reference, and the 2-ΔΔCt method was used to calculate the relative change in target gene expression.

Statistical Analysis

SPSS 22.0 (Chicago, IL) was used to analyse the data. The data are expressed as the mean±standard deviation (SD). Differences among groups were analysed by ANOVA and a post hoc Tukey-Kramer test. Independent samples were analysed by Student's *t*-test. A P-value of < 0.05 was considered statistically significant.

Results

CS Causes Emphysema and Skeletal Muscle Atrophy

To investigate the effects of CS on the lungs and skeletal muscles of mice, we evaluated the body weight, gastrocnemius muscle weight, and pathology of the lungs and skeletal muscles. Both the body weight and gastrocnemius muscle weight were significantly decreased in the mice exposed to CS, while the mean alveolar intervals were significantly increased, compared with those of the control mice ($P<0.05$) (Figure 1A–C). We also measured the

Table 1 Primers Used for the Real Time-PCR

HDAC2: forward (5′-3′) AGCCCATGGCGTACAGTCAA, reverse(5′-3′)GGGATGACCCTGGCCATAATAA
MURF1: forward (5′-3′) ATCACGCAGGAGCAGGAGGAG, reverse(5′-3′) CTTGGCACTTGAGAGGAAGGTAGC
MAFbx: forward (5′-3′) TTCACAAAGGAAGTACGAAGGA, reverse(5′-3′)GCTGGTCTTCAAGAACTTTCAG
P53: forward (5′-3′) TGGAAGGAAATTTGTATCCCGA, reverse(5′-3′)GTGGATGGTGGTATACTCAGAG
P21: forward (5′-3′) ATGTCCAATCCTGGTGATGTC, reverse(5′-3′)GAAGTCAAAGTTCCACCGTTC
GAPDH: forward (5′-3′) TGTGTCCGTCGTGGATCTGA, reverse (5′-3′) TTGCTGTTGAAGTCGCAGGAG

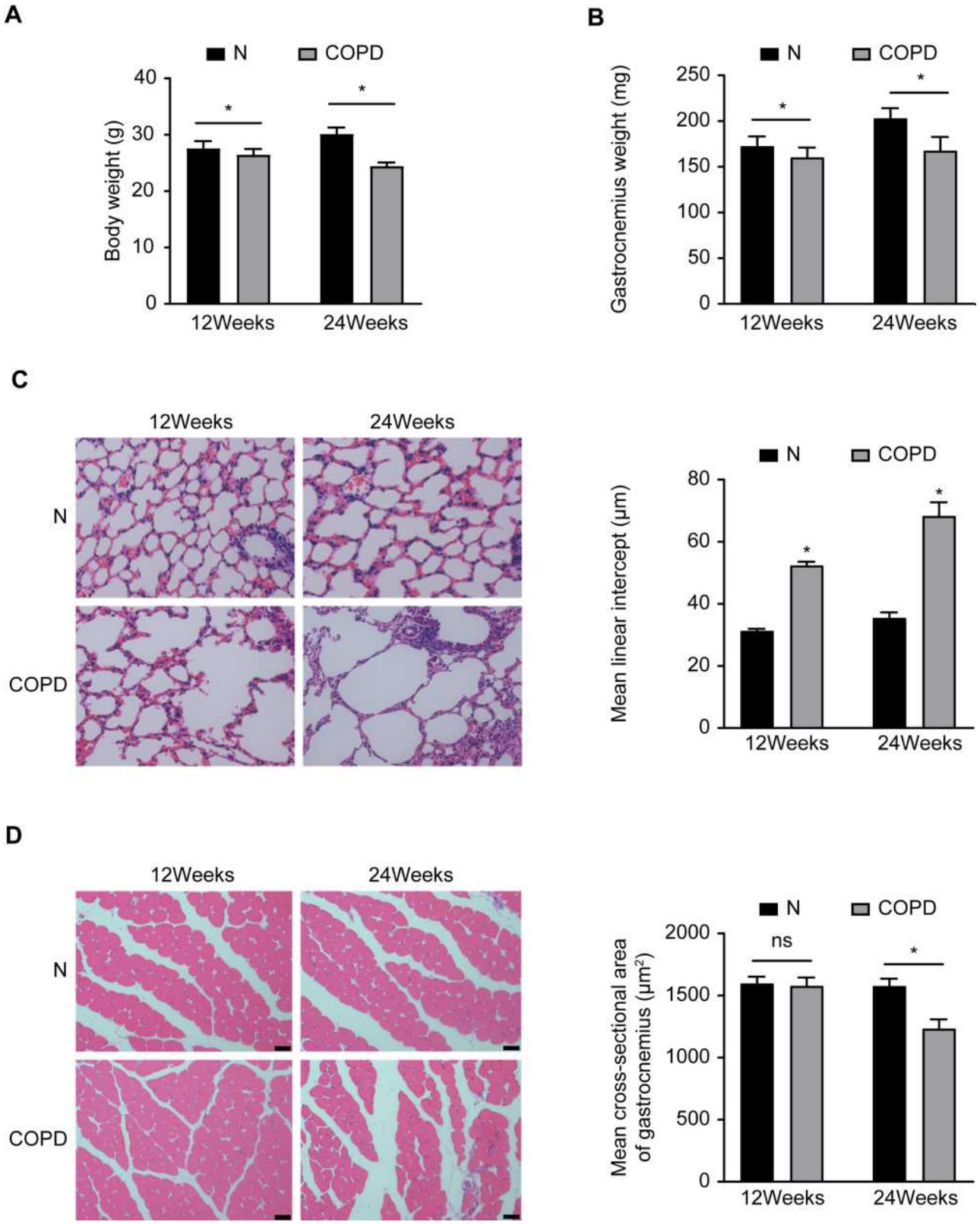

Figure 1 Chronic CS-induced emphysema and skeletal muscle atrophy in mice. (**A**) Body weight and gastrocnemius muscle (**B**) with or without CS exposure in mice. (**C**) Emphysema and skeletal muscle cross-sectional area (**D**) with or without CS exposure in mice. Data are representative images (magnification x 200) and expressed as the mean ± SD of each group (n=8) of mice. *p<0.05 vs control group (N).

cross-sectional areas of the gastrocnemius muscles, which did not significantly change after 12 weeks of CS exposure and significantly decreased after 24 weeks of CS exposure compared with the control treatment ($P<0.05$) (Figure 1D). These results indicated that chronic CS exposure leads to the development of emphysema and skeletal muscle atrophy in mice leads to the development of emphysema and skeletal muscle atrophy in mice.

Decreased HDAC2 Expression and Increased Atrophy- and Senescence-Related Protein Expression in Mice with Emphysema

Compared with the control group, the COPD group exhibited significantly decreased protein levels of HDAC2 and the senescence marker SMP30, while the expression of atrophy-related proteins (MURF1 and MAFbx) and senescence-related proteins (P53 and P21) was significantly increased in the gastrocnemius muscle ($P<0.05$) (Figure 2A and B). These results showed that chronic CS exposure decreases HDAC2 expression and enhances skeletal muscle atrophy and senescence in the gastrocnemius muscle.

CSE Induces Atrophy and Decreases HDAC2 Expression in C2C12 Cells

C2C12 cells can differentiate and form myotubes. To investigate the effect of CSE on myotube diameter, we examined the changes in myotube diameter in C2C12 myoblasts after treatment with different concentrations of CSE for 24 hours. The results showed that CSE led to myotube atrophy, and the myotube diameter significantly decreased as the CSE concentration increased in a concentration-dependent manner ($P<0.05$) (Figure 3A and B).

Moreover, the MURF1 and MAFbx protein levels were increased in C2C12 cells treated with CSE for 24 hours in a concentration-dependent manner ($P<0.05$). In addition, we also found that the HDAC2 protein levels exhibited an opposite trend with respect to the CSE concentrations ($P<0.05$) (Figure 3C). These results suggested that CSE caused myotube atrophy, which was accompanied by decreased HDAC2 protein levels.

Overexpression of HDAC2 Inhibits CSE-Induced Atrophy in C2C12 Cells

To further investigate whether HDAC2 is associated with CSE-induced atrophy, we established C2C12 cells stably overexpressing HDAC2 by lentiviral transduction with LV-HDAC2 (or LV-NC as the control) and then simultaneously stimulated the cells with or without 0.3% CSE for 24 hours. The HDAC2 protein levels were significantly increased in the LV-HDAC2 group compared with the control (N) and negative control (LV-NC) groups, and the real-time PCR results were consistent with the protein results, suggesting that HDAC2 was successfully overexpressed ($P<0.05$) (Figure 4A).

Next, we detected the changes in myotube diameter by cellular immunofluorescence. The results showed that compared with the LV-NC group, the LV-NC and LV-HDAC2 overexpression groups exhibited significantly decreased myotube diameters after CSE treatment ($P<0.05$); however, compared with the LV-NC group treated with CSE, the HDAC2 overexpression group exhibited increased the myotube diameters ($P<0.05$) (Figure 4B). We also examined the changes in the protein and mRNA expression of MURF1 and MAFbx. The results showed that the MURF1 and MAFbx protein and mRNA expression levels in the LV-NC and LV-HDAC2 groups treated with CSE were significantly higher than those in the control LV-NC group ($P<0.05$) (Figure 4C and D). These results suggested that CSE-induced atrophy is associated with HDAC2 and that overexpression of HDAC2 ameliorates myotube atrophy.

Overexpression of HDAC2 Ameliorates CSE-Induced Senescence in C2C12 Cells

In a previous study, we found that HDAC2 mediates the inflammatory response in C2C12 cells,[19] and inflammation can lead to senescence. To investigate whether HDAC2 is involved in the cellular senescence induced by CSE, we first detected the changes in the cellular senescence of each group by β-galactose. The results showed that senescence was significantly increased in the LV-NC group and group after CSE treatment compared with the control LV-NC group ($P<0.05$). In contrast, senescence was decreased in the LV-HDAC2 group treated with CSE compared with the LV-NC group treated with CSE ($P<0.05$) (Figure 5A). The expression of senescence-related proteins was also examined. The results showed that the expression of P53 and P21 was significantly increased at both the protein and mRNA levels after treatment with CSE ($P<0.05$), whereas overexpression of HDAC2 inhibited the expression of P53 and P21 after treatment with CSE ($P<0.05$). In contrast,

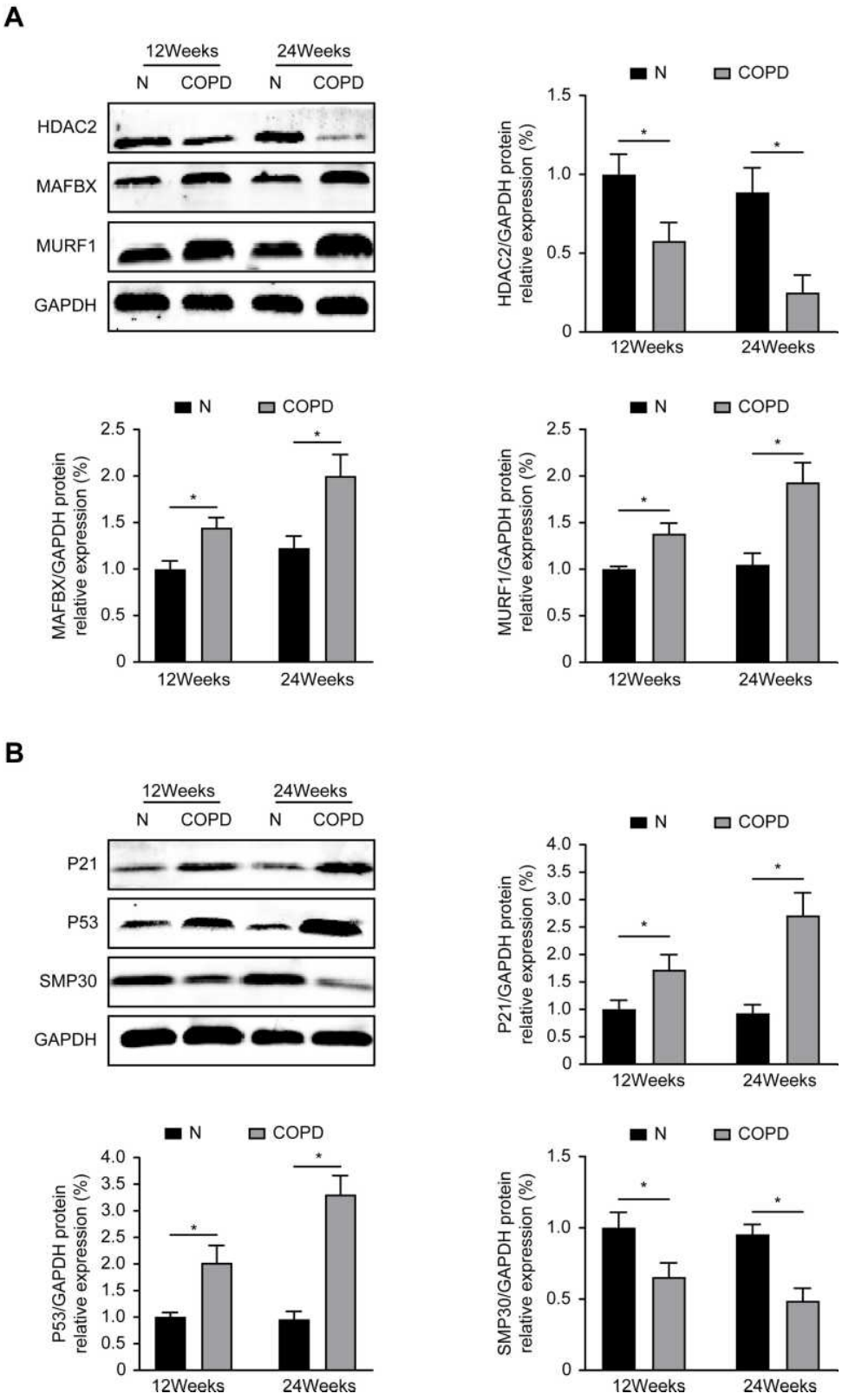

Figure 2 Atrophy and senescence-related protein expression in mice. (**A**) The atrophy-associated markers protein expression level of MURF1, MAFbx, HDAC2 after 12 and 24 weeks. (**B**) The senescence markers protein expression level of P53, P21, SMP30 after 12 and 24 weeks. Values are expressed as means±SD. Experiments were repeated 3 times with similar results. *p<0.05 vs control group (N).

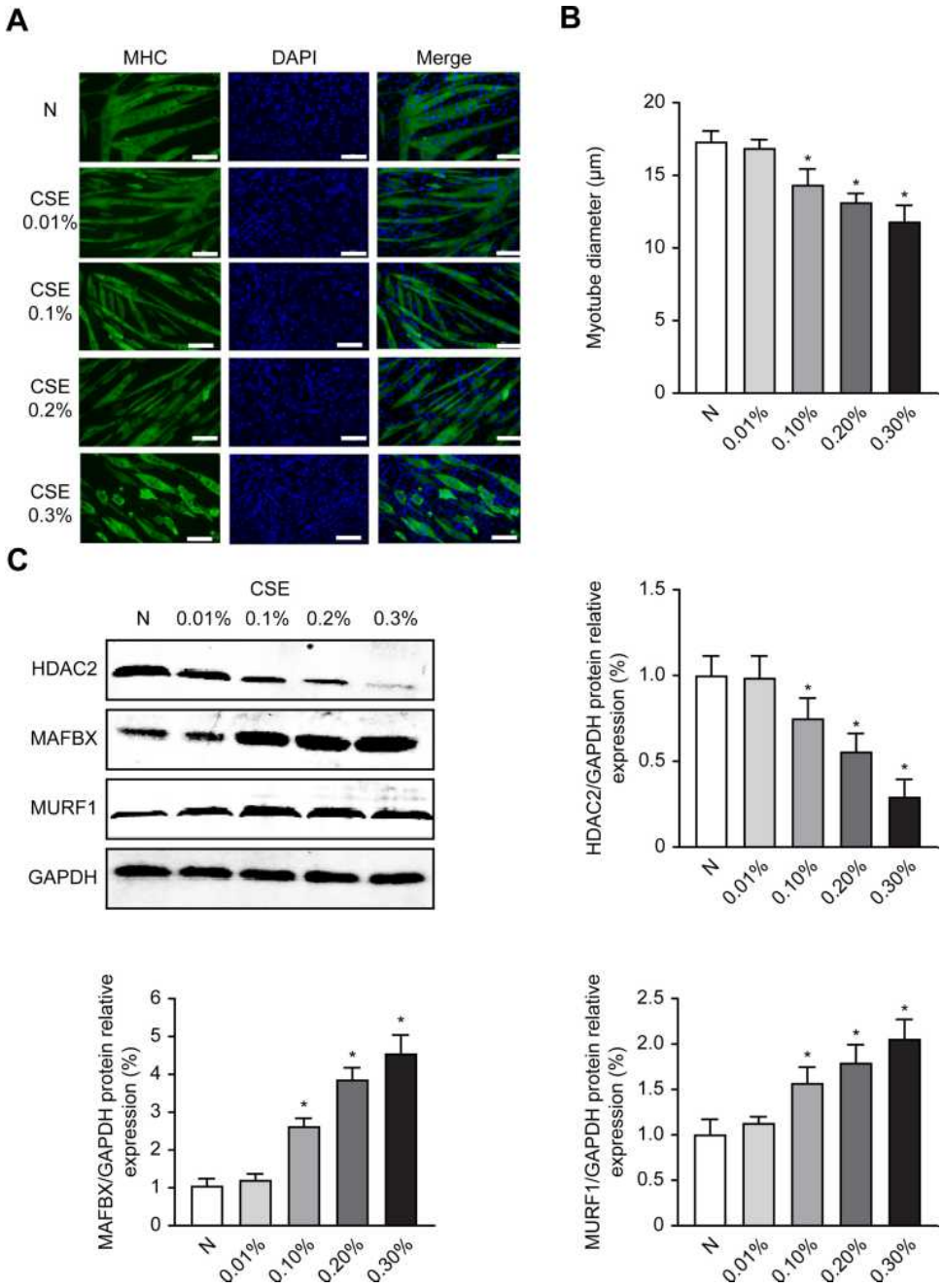

Figure 3 CSE decreases myotube diameter and increases atrophy-related proteins in C2C12 cells. After 6 days of cell differentiation and 24 hours of treatment with CSE, the morphological changes of the cells were observed, and Western analysis of the levels of MAFbx and MuRF1 protein expression was performed. (**A**) C2C12 myotubular phenotype changes after different CSE concentrations; 200×. (**B**) Measurements of average myotube diameter after 24 hours in different treatment groups exposed to CSE. (**C**) The protein expression level of MURF1, MAFbx and HDAC2 after 24 hours in different treatment groups exposed to CSE. Values are expressed as means±SD. Experiments were repeated 3 times with similar results. *p<0.05 vs control group (N).

the SMP30 protein levels showed an opposite trend to those of the P53 and P21 levels (P<0.05) (Figure 5B and C). In addition, the IKK and NF-Kβp65 protein levels were consistent with the cell senescence results (P<0.05) (Figure 5D). These results showed that CSE leads to cellular senescence and that overexpression of HDAC2 effectively ameliorates senescence.

HDAC2 Mediates CSE-Induced Skeletal Muscle Atrophy and Senescence via the NF-κB Pathway

We wanted to determine whether HDAC2 and the NF-κB pathway are involved in the skeletal muscle atrophy and senescence induced by CSE. C2C12 cells were pretreated

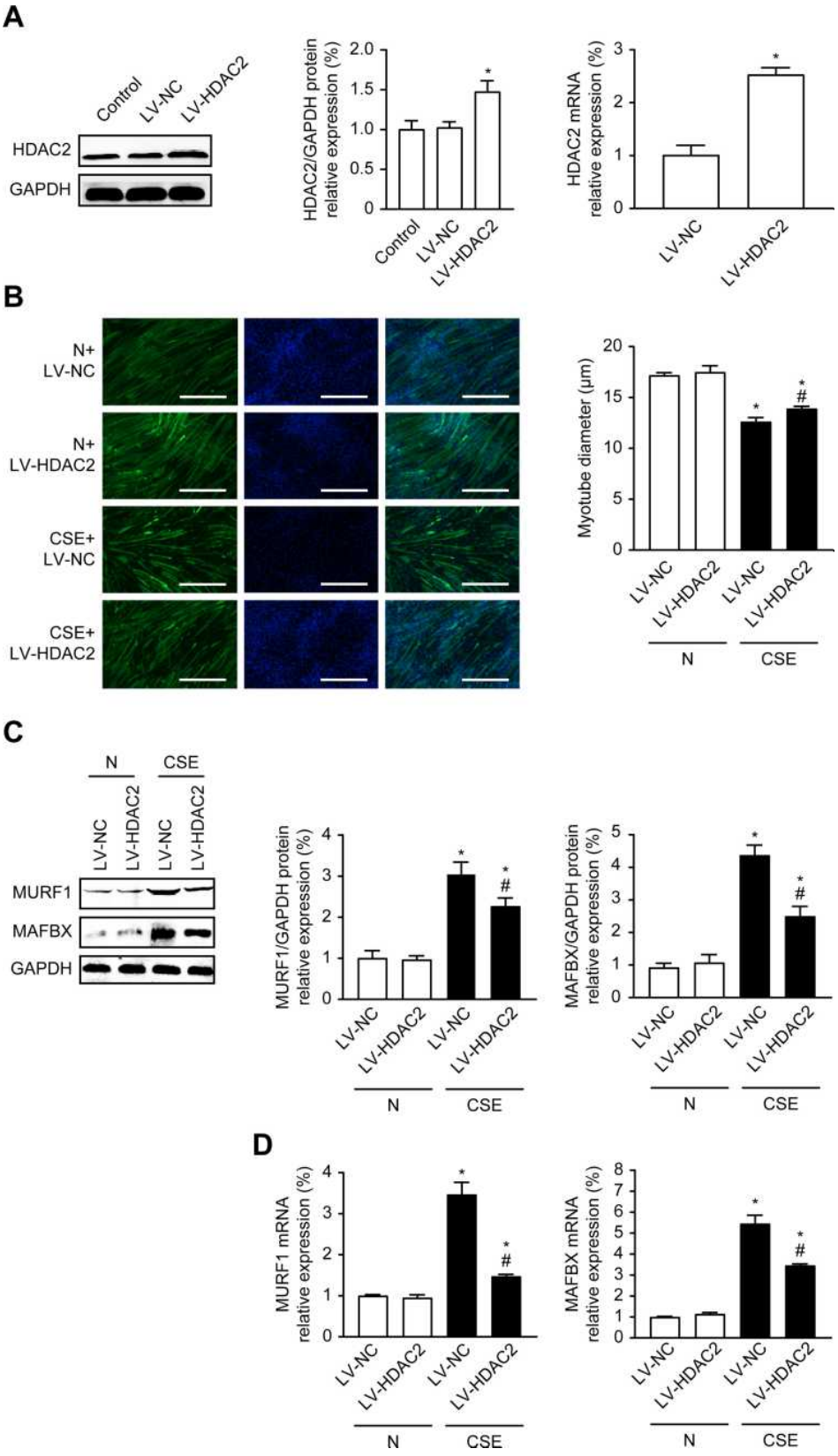

Figure 4 Overexpression of HDAC2 inhibits CSE-induced atrophy in C2C12 cells. (**A**) Effects of LV-HDAC2 Overexpression on HDAC2 Protein and mRNA. (**B**) Immunofluorescence measurement of the mean myotube diameter after 24 hours of 0.3% CSE between the different groups; 100×. (**C**) The protein expression level of MURF1, MAFbx, HDAC2 in cells with or without 0.3% CSE. (**D**) The mRNA level of MURF1, MAFbx in cells with or without 0.3% CSE. Values are expressed as means±SD. Experiments were repeated 3 times with similar results. *p<0.05 vs control NC group (LV-NC), #p<0.05 vs CSE+LV-NC group.

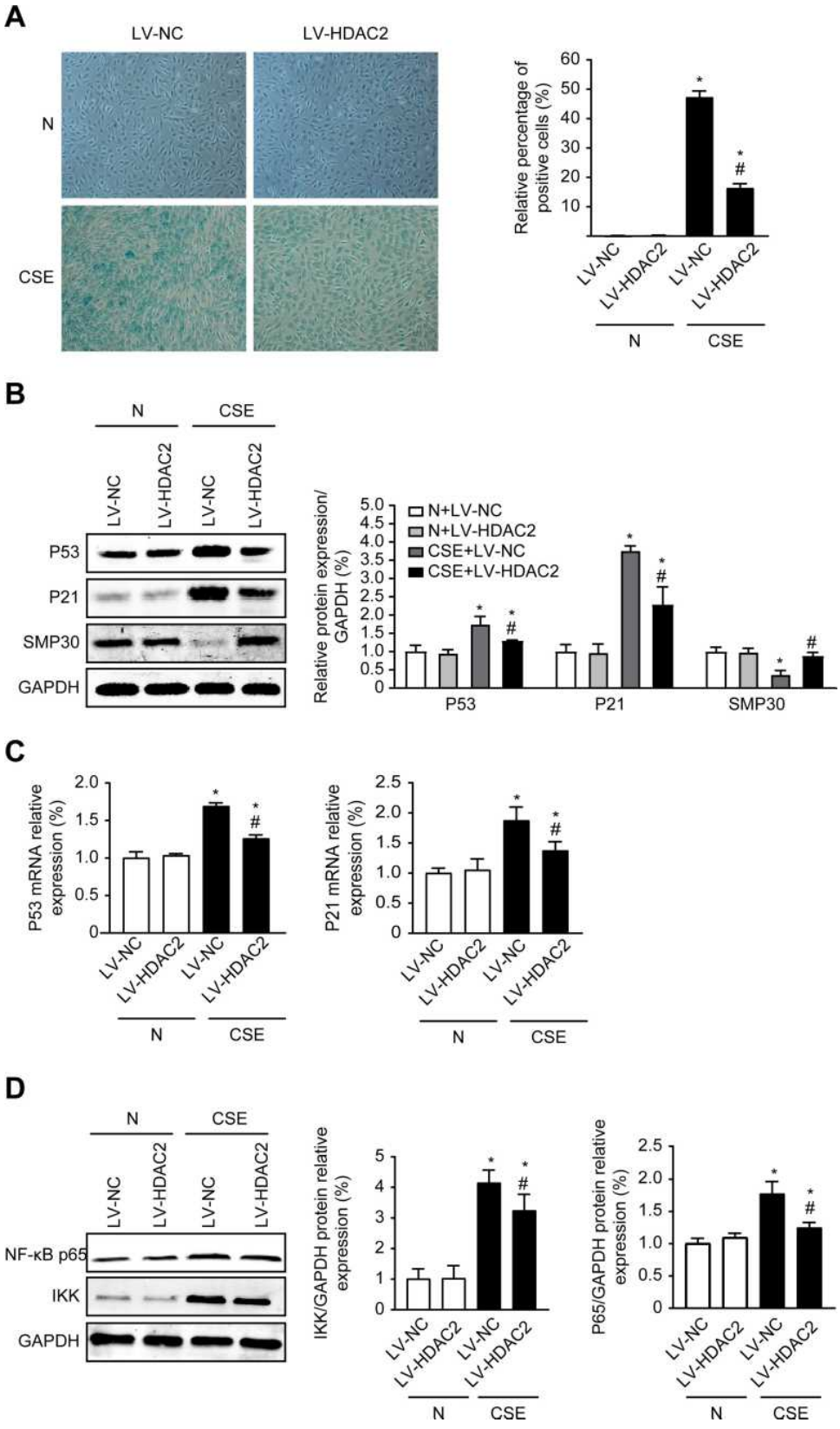

Figure 5 Overexpression of HDAC2 Inhibits Senescence in C2C12 Cells. (**A**) β-Galactosidase staining measurement of cellular senescence after 24 hours of 0.3% CSE between the different groups, 100×. (**B**) The protein expression level of P53, P21, SMP30 in cells with or without 0.3% CSE. (**C**) The mRNA level of P53, P21 in cells with or without 0.3% CSE. (**D**) The protein expression level of NF-κBp65 and IKK in cells with or without 0.3% CSE. Values are expressed as means±SD. Experiments were repeated 3 times with similar results. *p<0.05 vs control NC group (LV-NC), #p<0.05 vs CSE+LV-NC group.

with 20 μM PDTC, and then, the cells were incubated with CSE for 24 hours. The results indicated that the NF-κB p65 protein levels were significantly reduced in the cells overexpressing HDAC2 or treated with PDTC compared to the cells exposed to CSE alone ($P<0.05$), and the NF-κBp65 protein levels were significantly reduced after both HDAC2 overexpression and PDTC treatment compared to either HDAC2 overexpression or PDTC treatment alone in cells exposed to CSE ($P<0.05$) (Figure 6A).

Compared with exposure to CSE alone, overexpression of HDAC2 or treatment with PDTC in cells exposure to CSE resulted in significantly increased myotube diameters ($P<0.05$), and the myotube diameters were significantly increased after both the overexpression of HDAC2 and treatment with PDTC compared with either the overexpression of HDAC2 or treatment with PDTC alone in cells exposed to CSE ($P<0.05$) (Figure 6B). In addition, we found that overexpression of HDAC2 or treatment with PDTC alone significantly decreased the protein levels of P53 and P21 compared to exposure to CSE alone ($P<0.05$). In contrast, overexpression of HDAC2 and treatment with PDTC further decreased the protein levels of P53 and P21 ($P<0.05$) (Figure 6C). These results suggested that CSE causes atrophy and senescence via the HDAC2/NF-κB pathway.

Discussion

Skeletal muscle dysfunction (SMD) is a relevant comorbidity associated with poor outcomes in COPD patients, including greater hospitalization rates, worse quality of life, and lower survival.In the present study, we found that HDAC2 reverses CS-induced atrophy and senescence by regulating the NF-κB signalling pathway. These data suggested that the HDAC2/NF-κB signalling pathways may be a promising target for effective new SMD treatments in patients with CS-induced emphysema or COPD. However, previous studies have mainly focused on the role of HDAC2 in skeletal muscle inflammation, and few studies have addressed the role of HDAC2 in skeletal muscle atrophy and senescence.

In recent years, it has been demonstrated that SMD during COPD is associated with physical inactivity, nutritional abnormalities, hormonal changes, systemic inflammation, and oxidative stress.[16,34] Doucet found that the mRNA expression the muscle-specific E3s MURF1 and MAFbx was increased in the quadriceps muscles of COPD patients compared with the quadriceps muscles of healthy subjects.[35] In addition, Vogiatzis and colleagues[36] found that compared with those of noncachectic COPD patients, the protein levels of MAFbx in the vastus lateralis muscles of cachectic COPD patients were significantly increased. In the present study, we found that CS causes atrophy, which is accompanied by the increased expression of MURF1 and MAFbx in mouse gastrocnemius muscles.

Sarcopenia is characterized by both loss and atrophy of muscle cells, and its molecular mechanisms are related to cellular senescence.[37] Hallmarks of senescence include telomere shortening, genomic instability, epigenetic alterations, disrupted protein homeostasis, mitochondrial dysfunction, and nutrient sensing dysregulation, all of which can be observed in patients with COPD.[38] Oxidative stress directly induces cell cycle arrest by causing DNA damage and activating P53 and P21 in COPD.[39] In addition, SMP30 is an age-related multifunctional protein that is closely associated with lung cell senescence in the mouse COPD model.[40] The present study demonstrated an increase in the expression of the senescence-associated proteins P53 and P21 and a decrease in the expression of SMP30 in the gastrocnemius muscles of mice exposed to CS.

There is growing evidence that indicates that HDAC2 promotes repair during DNA damage and regulates cellular senescence and inflammation by deacetylating histones and transcription factors (eg, NF-κB).[41] Specific knockdown of HDAC1/2 in skeletal muscle resulted in progressive sarcopathy in mice.[42] In addition, a significant decrease in HDAC2 expression was observed in the quadriceps muscles of patients with COPD.[29] In the present study, we observed the decreased expression of HDAC2 in C2C12 cells treated with CSE, which was consistent with the in vivo data. To further investigate the role of HDAC2 in atrophy and senescence, we overexpressed HDAC2 in C2C12 cells. Overexpression of HDAC2 significantly ameliorated the CSE-induced myotube atrophy and senescence and reversed the increased MURF1, MAFbx, P53, and P21 expression at both the protein and mRNA levels. These results indicated that HDAC2 plays an essential role in CS-induced skeletal muscle atrophy and senescence.

The NF-κB signalling pathway in the skeletal muscles of COPD patients regulates the expression of inflammatory cytokines, antioxidants, and stress proteins, impairing muscle motility.[37,43] Increased expression of NF-κB in skeletal muscle can lead to the upregulation of MuRF1 expression and enhanced catabolism of myosin, resulting in the loss of muscle components. In contrast, blocking NF-κB can prevent muscle atrophy.[44] Cai et al[45] found that activation of IKK-β

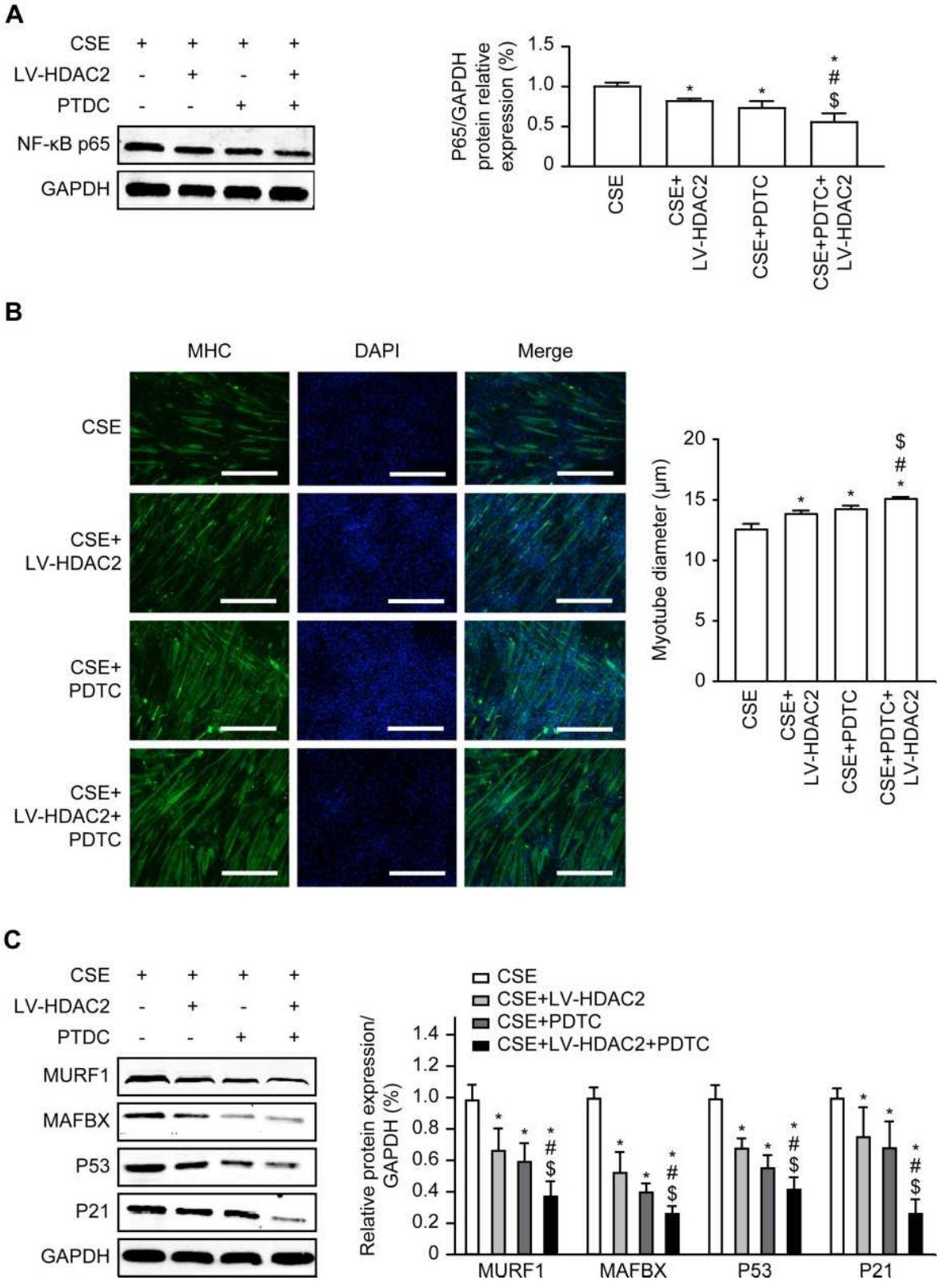

Figure 6 Effects of NF-κB pathway on HDAC2-regulated atrophy and senescence in C2C2 cells. (**A**) Western blot assays for NF-κBp65 expression after overexpression of HDAC2 and PDTC in CSE. (**B**) Immunofluorescence detection of myotube diameter, 100×. (**C**) Western blot assays for MURF1, MAFbx, P53, and P21. Values are expressed as means±SD. Experiments were repeated 3 times with similar results. *$p<0.05$ vs CSE group, #$p<0.05$ vs CSE+LV-HDAC2 group, $$p<0.05$ vs CSE+PDTC group.

in muscle-specific IKK-β transgenic mice (MIKK) significantly induced skeletal muscle atrophy, while its inhibition reversed muscle atrophy. In MuRF-1-/- mice, muscle atrophy was significantly reduced, demonstrating that transcriptional activation of MuRF-1 by NF-kB is a key step in the induction of skeletal muscle atrophy by NF-κB. In a previous study, we found that CS inhibits HDAC2 expression, which is negatively correlated with NF-κB expression and activity.[19] In addition, the accumulation of senescent cells triggers chronic inflammation, and the NF-κB signalling pathway plays an essential role in this process.[46] However, it is unclear whether HDAC2 can mediate CS-induced skeletal muscle atrophy and senescence via the NF-κB signalling pathway. In the present study, we found that the overexpression of HDAC2 significantly reduced the NF-κB and IKK protein levels compared with CSE alone, suggesting that the NF-κB pathway may be involved in CSE-induced atrophy and senescence in C2C12 cells. To further investigate the effects of HDAC2 and the NF-κB signalling pathway on atrophy and senescence, C2C12 cells were pretreated with the NF-κB-specific inhibitor PDTC (20 μM) for 2 hours before CSE treatment. The results showed that the effects of CSE on C2C12 cell atrophy and senescence could be significantly reversed by PDTC, and the inhibitory effect was even more obvious when the cells were treated with PDTC and overexpressed HDAC2. These results suggested that HDAC2 and the NF-κB signalling pathway are involved in atrophy and senescence.

The major limitations of this study are as follows. 1) We did not use the HDAC2-knockout mouse model, which may limit the functional studies of this molecule in animal experiments. Further research is required to observe the effects of HDAC2 on CS-induced skeletal muscle atrophy in vivo using HDAC2 inhibitors or HDAC2-knockout mice. 2) Trichostatin A (TSA), an HDAC inhibitor, blocks CS-induced skeletal muscle atrophy and histomorphological changes.[47] This finding indicates that the use of HDAC2 as a target for the treatment of skeletal muscle atrophy remains controversial, and this topic may require additional experimental support. 3) This study only included in vivo and in vitro experiments and lacks reliable clinical evidence; therefore, these findings still need to be combined with bioinformatics analysis and further validated in clinical subjects.

Conclusion

In conclusion, our data suggested that HDAC2 is involved in CS-induced skeletal muscle atrophy and senescence by regulating the NF-κB signalling pathway. This study helps to further understand the pathogenesis of skeletal muscle dysfunction in COPD.

Abbreviations

HDAC2, histone deacetylase 2; CSE, cigarette smoke extract; CS, cigarette smoking; MURF1, muscle ring finger gene 1; MAFbx, muscle atrophy F-box; SMP30, senescence marker protein-30.

Ethics Approval and Consent to Participate

All animal experiments were conducted in accordance with the Guide for the Care and Use of Laboratory Animals and approved by the Institutional Animal Care Committee (IACUC), an organization accredited by the International Association for the Assessment and Accreditation of Laboratory Animal Care in China and the Guangxi Medical University Laboratory Animal Committee (No.201911013).

Acknowledgments

This work was supported by the National Natural Science Foundation of China (81560008, 81960010), Innovation Project of Guangxi Graduate Education (YCBZ2020044), and Natural Science Foundation of Guangxi (2017JJA10229, 2018JJA140868).

Disclosure

The authors declare no conflict of interest.

References

1. Vanfleteren L, Spruit MA, Wouters EFM, Franssen FME. Management of chronic obstructive pulmonary disease beyond the lungs. *Lancet Respirat Med*. 2016;4(11):911–924. doi:10.1016/S2213-2600(16)00097-7
2. Barreiro E, Gea J. Molecular and biological pathways of skeletal muscle dysfunction in chronic obstructive pulmonary disease. *Chron Respir Dis*. 2016;13(3):297–311. doi:10.1177/1479972316642366
3. Seymour JM, Spruit MA, Hopkinson NS, et al. The prevalence of quadriceps weakness in COPD and the relationship with disease severity. *Eur Respir J*. 2010;36(1):81–88. doi:10.1183/09031936.00104909
4. Degens H, Gayan-Ramirez G, van Hees HW. Smoking-induced skeletal muscle dysfunction: from evidence to mechanisms. *Am J Respir Crit Care Med*. 2015;191(6):620–625. doi:10.1164/rccm.201410-1830PP
5. Simoes DCM, Vogiatzis I. Can muscle protein metabolism be specifically targeted by exercise training in COPD? *J Thorac Dis*. 2018;10(Suppl 12):S1367–s1376. doi:10.21037/jtd.2018.02.67
6. Verreijen AM, Verlaan S, Engberink MF, Swinkels S, de Vogel-van den Bosch J, Weijs PJ. A high whey protein-, leucine-, and vitamin D-enriched supplement preserves muscle mass during intentional weight loss in obese older adults: a double-blind randomized controlled trial. *Am J Clin Nutr*. 2015;101(2):279–286. doi:10.3945/ajcn.114.090290

7. Abdellaoui A, Préfaut C, Gouzi F, et al. Skeletal muscle effects of electrostimulation after COPD exacerbation: a pilot study. *Eur Respir J*. 2011;38(4):781–788. doi:10.1183/09031936.00167110
8. Kirkham PA, Barnes PJ. Oxidative stress in COPD. *Chest*. 2013;144 (1):266–273. doi:10.1378/chest.12-2664
9. Jaitovich A, Barreiro E. Skeletal muscle dysfunction in chronic obstructive pulmonary disease. What we know and can do for our patients. *Am J Respir Crit Care Med*. 2018;198(2):175–186. doi:10.1164/rccm.201710-2140CI
10. Wilkinson DJ, Piasecki M, Atherton PJ. The age-related loss of skeletal muscle mass and function: measurement and physiology of muscle fibre atrophy and muscle fibre loss in humans. *Ageing Res Rev*. 2018;47:123–132. doi:10.1016/j.arr.2018.07.005
11. Plant PJ, Brooks D, Faughnan M, et al. Cellular markers of muscle atrophy in chronic obstructive pulmonary disease. *Am J Respir Cell Mol Biol*. 2010;42(4):461–471. doi:10.1165/rcmb.2008-0382OC
12. Schiaffino S, Dyar KA, Ciciliot S, Blaauw B, Sandri M. Mechanisms regulating skeletal muscle growth and atrophy. *FEBS J*. 2013;280 (17):4294–4314. doi:10.1111/febs.12253
13. Hussain SN, Sandri M. Role of autophagy in COPD skeletal muscle dysfunction. *J Appl Physiol*. 2013;114(9):1273–1281. doi:10.1152/japplphysiol.00893.2012
14. Bodine SC, Baehr LM. Skeletal muscle atrophy and the E3 ubiquitin ligases MuRF1 and MAFbx/atrogin-1. *Am J Physiol Endocrinol Metab*. 2014;307(6):E469–484. doi:10.1152/ajpendo.00204.2014
15. Bodine SC, Latres E, Baumhueter S, et al. Identification of ubiquitin ligases required for skeletal muscle atrophy. *Science*. 2001;294 (5547):1704–1708. doi:10.1126/science.1065874
16. Rom O, Reznick AZ. The role of E3 ubiquitin-ligases MuRF-1 and MAFbx in loss of skeletal muscle mass. *Free Radic Biol Med*. 2016;98:218–230. doi:10.1016/j.freeradbiomed.2015.12.031
17. Foletta VC, White LJ, Larsen AE, Leger B, Russell AP. The role and regulation of MAFbx/atrogin-1 and MuRF1 in skeletal muscle atrophy. *Pflugers Arch*. 2011;461(3):325–335. doi:10.1007/s00424-010-0919-9
18. Huang D, Ma Z, He Y, et al. Long-term cigarette smoke exposure inhibits histone deacetylase 2 expression and enhances the nuclear factor-κB activation in skeletal muscle of mice. *Oncotarget*. 2017;8 (34):56726–56736. doi:10.18632/oncotarget.18089
19. Bin Y, Xiao Y, Huang D, et al. Theophylline inhibits cigarette smoke-induced inflammation in skeletal muscle by upregulating HDAC2 expression and decreasing NF-κB activation. *Am J Physiol Lung Cell Mol Physiol*. 2019;316(1):L197–l205. doi:10.1152/ajplung.00005.2018
20. Rajendrasozhan S, Yao H, Rahman I. Current perspectives on role of chromatin modifications and deacetylases in lung inflammation in COPD. *Copd*. 2009;6(4):291–297. doi:10.1080/15412550903049132
21. Gong F, Miller KM. Mammalian DNA repair: HATs and HDACs make their mark through histone acetylation. *Mutat Res*. 2013;750 (1–2):23–30. doi:10.1016/j.mrfmmm.2013.07.002
22. Barnes PJ. Histone deacetylase-2 and airway disease. *Ther Adv Respir Dis*. 2009;3(5):235–243. doi:10.1177/1753465809348648
23. Tan C, Xuan L, Cao S, Yu G, Hou Q, Wang H. Decreased histone deacetylase 2 (HDAC2) in peripheral blood monocytes (PBMCs) of COPD patients. *PLoS One*. 2016;11(1):e0147380. doi:10.1371/journal.pone.0147380
24. Kim RY, Horvat JC, Pinkerton JW, et al. MicroRNA-21 drives severe, steroid-insensitive experimental asthma by amplifying phosphoinositide 3-kinase-mediated suppression of histone deacetylase 2. *J Allergy Clin Immunol*. 2017;139(2):519–532. doi:10.1016/j.jaci.2016.04.038
25. Singh T, Prasad R, Katiyar SK. Inhibition of class I histone deacetylases in non-small cell lung cancer by honokiol leads to suppression of cancer cell growth and induction of cell death in vitro and in vivo. *Epigenetics*. 2013;8(1):54–65. doi:10.4161/epi.23078
26. Korfei M, Skwarna S, Henneke I, et al. Aberrant expression and activity of histone deacetylases in sporadic idiopathic pulmonary fibrosis. *Thorax*. 2015;70(11):1022–1032. doi:10.1136/thoraxjnl-2014-206411
27. Yao H, Rahman I. Role of histone deacetylase 2 in epigenetics and cellular senescence: implications in lung inflammaging and COPD. *Am J Physiol Lung Cell Mol Physiol*. 2012;303(7):L557–L566. doi:10.1152/ajplung.00175.2012
28. Barnes PJ, Adcock IM, Ito K. Histone acetylation and deacetylation: importance in inflammatory lung diseases. *Eur Respir J*. 2005;25 (3):552–563. doi:10.1183/09031936.05.00117504
29. To M, Swallow EB, Akashi K, et al. Reduced HDAC2 in skeletal muscle of COPD patients. *Respir Res*. 2017;18(1):99. doi:10.1186/s12931-017-0588-8
30. Gosker HR, Langen RC, Bracke KR, et al. Extrapulmonary manifestations of chronic obstructive pulmonary disease in a mouse model of chronic cigarette smoke exposure. *Am J Respir Cell Mol Biol*. 2009;40(6):710–716. doi:10.1165/rcmb.2008-0312OC
31. Caron AZ, Haroun S, Leblanc E, et al. The proteasome inhibitor MG132 reduces immobilization-induced skeletal muscle atrophy in mice. *BMC Musculoskelet Disord*. 2011;12:185. doi:10.1186/1471-2474-12-185
32. Qiu SL, Duan MC, Liang Y, et al. Cigarette smoke induction of interleukin-27/WSX-1 regulates the differentiation of Th1 and Th17 cells in a smoking mouse model of emphysema. *Front Immunol*. 2016;7:553. doi:10.3389/fimmu.2016.00553
33. Mercado N, To Y, Ito K, Barnes PJ. Nortriptyline reverses corticosteroid insensitivity by inhibition of phosphoinositide-3-kinase-δ. *J Pharmacol Exp Ther*. 2011;337(2):465–470. doi:10.1124/jpet.110.175950
34. Debigaré R, Marquis K, Côté CH, et al. Catabolic/anabolic balance and muscle wasting in patients with COPD. *Chest*. 2003;124 (1):83–89. doi:10.1378/chest.124.1.83
35. Doucet M, Russell AP, Léger B, et al. Muscle atrophy and hypertrophy signaling in patients with chronic obstructive pulmonary disease. *Am J Respir Crit Care Med*. 2007;176(3):261–269. doi:10.1164/rccm.200605-704OC
36. Vogiatzis I, Simoes DC, Stratakos G, et al. Effect of pulmonary rehabilitation on muscle remodelling in cachectic patients with COPD. *Eur Respir J*. 2010;36(2):301–310. doi:10.1183/09031936.00112909
37. Aversa Z, Zhang X, Fielding RA, Lanza I, LeBrasseur NK. The clinical impact and biological mechanisms of skeletal muscle aging. *Bone*. 2019;127:26–36. doi:10.1016/j.bone.2019.05.021
38. MacNee W. Is chronic obstructive pulmonary disease an accelerated aging disease? *Ann Am Thorac Soc*. 2016;13(Suppl 5):S429–s437. doi:10.1513/AnnalsATS.201602-124AW
39. Barnes PJ, Baker J, Donnelly LE. Cellular senescence as a mechanism and target in chronic lung diseases. *Am J Respir Crit Care Med*. 2019;200(5):556–564. doi:10.1164/rccm.201810-1975TR
40. Sato T, Seyama K, Sato Y, et al. Senescence marker protein-30 protects mice lungs from oxidative stress, aging, and smoking. *Am J Respir Crit Care Med*. 2006;174(5):530–537. doi:10.1164/rccm.200511-1816OC
41. Wilting RH, Yanover E, Heideman MR, et al. Overlapping functions of Hdac1 and Hdac2 in cell cycle regulation and haematopoiesis. *EMBO J*. 2010;29(15):2586–2597. doi:10.1038/emboj.2010.136
42. Moresi V, Carrer M, Grueter CE, et al. Histone deacetylases 1 and 2 regulate autophagy flux and skeletal muscle homeostasis in mice. *Proc Natl Acad Sci U S A*. 2012;109(5):1649–1654. doi:10.1073/pnas.1121159109
43. Remels AH, Gosker HR, Langen RC, et al. Classical NF-κB activation impairs skeletal muscle oxidative phenotype by reducing IKK-α expression. *Biochim Biophys Acta*. 2014;1842(2):175–185. doi:10.1016/j.bbadis.2013.11.001

44. Glass DJ. Skeletal muscle hypertrophy and atrophy signaling pathways. *Int J Biochem Cell Biol*. 2005;37(10):1974–1984. doi:10.1016/j.biocel.2005.04.018
45. Cai D, Frantz JD, Tawa NE, et al. IKKbeta/NF-kappaB activation causes severe muscle wasting in mice. *Cell*. 2004;119(2):285–298. doi:10.1016/j.cell.2004.09.027
46. Wei W, Ji S. Cellular senescence: molecular mechanisms and pathogenicity. *J Cell Physiol*. 2018;233(12):9121–9135. doi:10.1002/jcp.26956
47. Ding J, Li F, Cong Y, et al. Trichostatin A inhibits skeletal muscle atrophy induced by cigarette smoke exposure in mice. *Life Sci*. 2019;235:116800. doi:10.1016/j.lfs.2019.116800